ARTICLE
Journal of Cellular Biochemistry 115:1877–1887 (2014)

Journal of Cellular Biochemistry

A Phenolic Acid Phenethyl Urea Derivative Protects Against Irradiation-Induced Osteoblast Damage by Modulating Intracellular Redox State

Kyoung A. Kim,[1] Sung-Ho Kook,[2] Ji-Hye Song,[2] and Jeong-Chae Lee[2,3]*

[1]*Department of Oral and Maxillofacial Radiology and Research Institute of Clinical Medicine, Chonbuk National University, Jeonju 561-756, South Korea*

[2]*Department of Orthodontics and Institute of Oral Biosciences, Chonbuk National University, Jeonju 561-756, South Korea*

[3]*Research Center of Bioactive Materials, Chonbuk National University, Jeonju 561-756, South Korea*

ABSTRACT

Because irradiation may cause osteoradionecrosis, antioxidant supplementation is often used to suppress irradiation-mediated injury. This study examined whether a synthetic phenethyl urea compound, (*E*)-1-(3,4-dihydroxyphenethyl)-3-(3,4-dihydroxystyryl)urea (DPDS-U), prevents irradiation-mediated cellular damage in MC3T3-E1 osteoblastic cells. A relatively high dose of irradiation (>4 Gy) decreased cell viability and proliferation and induced DNA damage and cell cycle arrest at the G_2/M phase with the attendant increase of cyclin B1. Irradiation with 8 Gy induced intracellular reactive oxygen species (ROS) production and lipid peroxidation, and reduced glutathione content and superoxide dismutase activity in the cells. These events were significantly suppressed by treatment with 200 μM DPDS-U or 5 mM *N*-acetyl cysteine (NAC). DPDS-U or irradiation alone significantly increased heme oxygenase-1 (HO-1) expression and nuclear factor E2 p45-related factor-2 (Nrf2) nuclear translocation. Interestingly, pretreatment with DPDS-U facilitated irradiation-induced activation of the Nrf2/HO-1 pathway. The potential of DPDS-U to mediate HO-1 induction and protect against irradiation-mediated cellular damage was almost completely attenuated by transient transfection with Nrf2-specific siRNA or treatment with a pharmacological HO-1 inhibitor, zinc protoporphyrin IX. Additional experiments revealed that DPDS-U induced a radioprotective mechanism that differs from that induced by NAC through activation of Nrf2/HO-1 signaling. Collectively, our data suggest that DPDS-U-induced radioprotection is due to its dual function as an antioxidant to remove directly excessive intracellular ROS and as a prooxidant to stimulate intracellular redox-sensitive survival signal. J. Cell. Biochem. 115: 1877–1887, 2014.

KEY WORDS: IRRADIATION; OXIDATIVE STRESS; ANTIOXIDANT; HEME OXYGENASE-1; NUCLEAR FACTOR E2 P45-RELATED FACTOR 2

Humans are constantly exposed to ionizing radiation from natural and artificial sources. Radiotherapy in combination with surgery is a useful treatment for patients suffering from cancers. However, therapeutic irradiation can cause irrecoverable damage to intact bone tissue, eventually leading to osteoradionecrosis and subsequent loss of bone mass and an increased risk of bone fracture [Schultze-Mosgau et al., 2005; King et al., 2010].

Numerous efforts have been undertaken to elucidate the mechanisms by which irradiation causes damage to cells and tissues. Oxidative stress caused by excessive generation of reactive oxygen species (ROS) is believed to be a predominant mediator of ionizing radiation-induced damage. α-Tocopherol succinate has been shown to protect mice from radiation-induced gastrointestinal damage [Singh et al., 2012] and dietary antioxidants improve animal survival after total-body X-ray irradiation [Wambi et al., 2008]. *N*-acetyl cysteine (NAC) also protects against irradiation-mediated damage [Ueno et al., 2001; Wambi et al., 2008]. These findings suggest that antioxidant compounds may protect cells against irradiation-induced injury. However, the mechanisms by which antioxidants exert radioprotective effects on osteoblasts are not completely understood.

Kyoung A. Kim and Sung-Ho Kook contributed equally to this work.

Grant sponsor: Ministry of Education, Science and Technology; Grant numbers: 2011-0010073, NRF-2012R1A1B6001778.

*Correspondence to: Prof. Jeong-Chae Lee, Department of Orthodontics and Institute of Oral Biosciences (BK21 program), Research Center of Bioactive Materials, Chonbuk National University, Jeonju 561-756, South Korea.
E-mail: leejc88@jbnu.ac.kr

Manuscript Received: 10 December 2013; Manuscript Accepted: 30 May 2014

Accepted manuscript online in Wiley Online Library (wileyonlinelibrary.com): 6 June 2014

DOI 10.1002/jcb.24857 • © 2014 Wiley Periodicals, Inc.

Accumulating evidence has highlighted phenolic acids as major compounds responsible for plant-based beneficial activities. Considering that the antioxidant potential of phenolic acids is closely correlated with various biological, pharmacological, and medicinal abilities, our efforts have focused on the development of phenolic acid derivatives with stronger antioxidant activities than their corresponding phenolic acids. We previously synthesized phenolic acid phenethyl ureas (PAPU) containing one aromatic hydroxyl group from phenolic acids by a Curtius rearrangement [Kim et al., 2009]. The PAPU compounds synthesized were: (*E*)-1-(3,4-dihydroxyphenethyl)-3-styrylurea (DPS-U), (*E*)-1-(3,4-dihydroxystyryl)-3-phenethylurea (DSP-U), (*E*)-1-(3,4-dihydroxystyryl)-3-(4-hydroxyphenethyl) urea (DSHP-U), (*E*)-1-(3,4-dihydrophenethyl)-(3,4-dihydroxystyryl) urea (DPDS-U), (*E*)-1-(4-methoxyphenethyl)-3-(4-methoxystyryl) urea (MPMS-U), and (*E*)-1-(3,4-dihydroxyphenethyl)-3-(4-hydroxystyryl) urea (DPHS-U) (Fig. 1A). We preliminary found that these compounds exert antioxidant potential. Some of the PAPU compounds inhibited inflammatory responses and induced apoptosis of cancer cells [Kim et al., 2009; Hwang et al., 2010; Yu et al., 2010]. Our recent study also highlighted the possibility that PAPU compounds are capable of inhibiting irradiation-mediated damage in osteoblasts [Kim et al., 2013].

The aim of this study was to confirm whether PAPU compounds protect against irradiation-mediated cellular damage. We also investigated the possible mechanisms by which these compounds exert radioprotection in osteoblasts using the antioxidant NAC for comparison because of its well-known radioprotective effects.

MATERIALS AND METHODS

CHEMICALS AND LABORATORY EQUIPMENT

Unless otherwise specified, chemicals and laboratory wares were purchased from Sigma Chemical Co. (St. Louis, MO) and Falcon Labware (Becton Dickinson, Franklin Lakes, NJ), respectively. PAPU compounds were dissolved in dimethylsulfoxide (DMSO) immediately before use.

CELL CULTURE AND TREATMENT

MC3T3-E1 cells (ATCC, CRL-2593) were cultured in alpha-minimum essential medium (α-MEM) supplemented with 10% fetal bovine

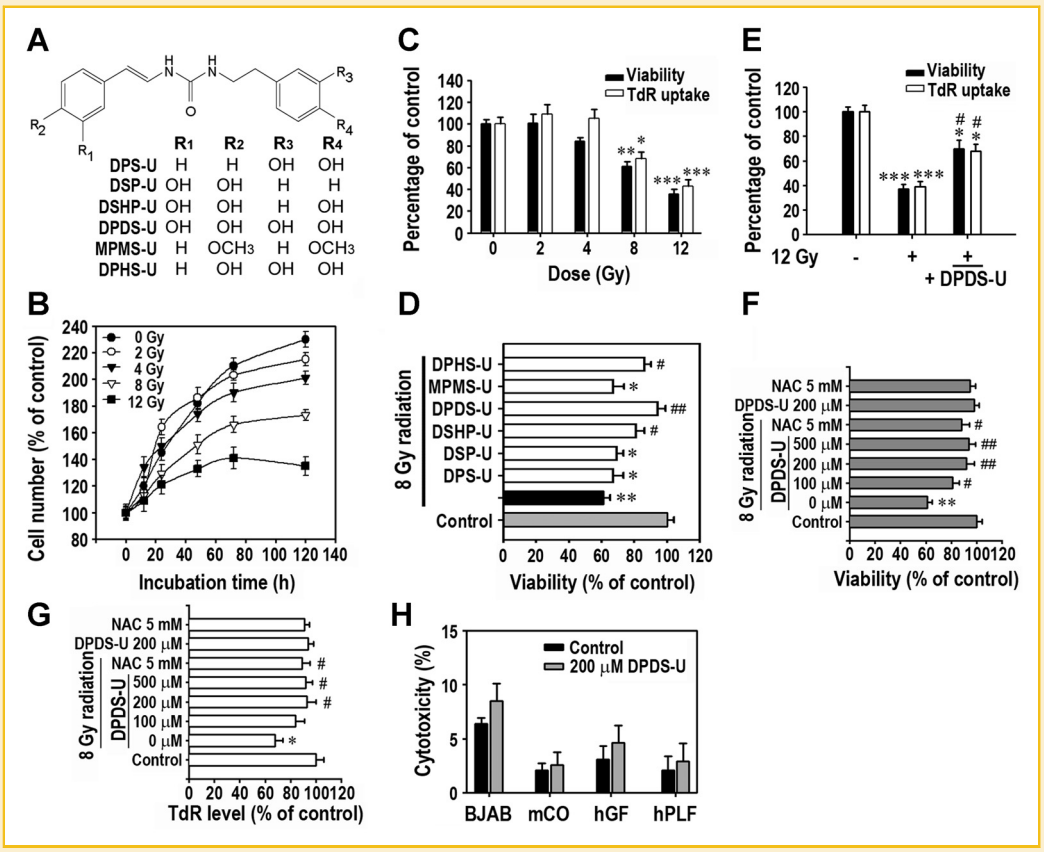

Fig. 1. Inhibitory effects of DPDS-U on radiation-mediated decreases in viability and DNA synthesis in MC3T3-E1 cells. A: Chemical structure of PAPU compounds. B: Cells were irradiated with the indicated doses (0–12 Gy) and counted after various times (0–120 h) of incubation. C: Cells were exposed to various doses (0–12 Gy) of radiation and cell viability and TdR uptake level were measured at 24 h post-irradiation. D: Cells were exposed to 8 Gy of radiation in the presence of each PAPU compound at 200 μM and analyzed by MTT assay at 24 h post-irradiation. Cells were irradiated with 12 Gy in the presence of 200 μM DPDS-U (E) or with 8 Gy in the presence of the indicated doses of DPDS-U or NAC (F,G) and viability and TdR uptake levels were determined at 24 h post-irradiation. H: Various types of cells including BJAB, mCO, hGF, and hPLF were treated with 200 μM DPDS-U alone for 24 h and then processed for trypan blue staining. $^{*}P < 0.05$, $^{**}P < 0.01$, and $^{***}P < 0.001$ versus non-irradiated control. $^{\#}P < 0.05$ and $^{\#\#}P < 0.01$ versus only irradiation.

serum (FBS; HyClone, Logan, UT) and antibiotics, as previously described [Son et al., 2006]. When the cells reached approximately 90% confuency in 6-well or 96-well culture plates they were exposed to various doses of irradiation or direct addition of H_2O_2. Unless otherwise specified, cells were treated with PAPU compounds or NAC 1 h before irradiation or exposure to a direct oxidative stress. BJAB cells and primary cultured cells (mouse calvarial osteoblasts, mCO; human gingival fibroblasts, hGF; human periodontal ligament fibroblasts, hPLF) were also incubated according to the methods described elsewhere [Son et al., 2006; 2009].

X-RAY IRRADIATION

MC3T3-E1 cells were exposed to various doses of radiation (0–12 Gy) at a rate of 1.5 Gy/min using a radiotherapeutic linear accelerator (Mevaprimus, Siemens, Munich, Germany). Because it has been suggested that FBS interferes with water radiolysis, the culture medium was replaced with α-MEM medium containing 0.5% FBS prior to irradiation. All irradiations were performed at room temperature and four culture plates were simultaneously exposed. Control samples were treated identically except that they received no irradiation.

MEASUREMENT OF VIABILITY, DNA SYNTHESIS, AND CELL NUMBER

These assays were performed according to methods described elsewhere [Son et al., 2006]. Briefly, the viability of cells was determined 24 h after irradiation by measuring their ability to reduce 3-(4,5-dimethylthiazol-2yl-)-2,5-diphenyl tetrazolium bromide (MTT). The proliferation rate was determined by measuring DNA synthesis using the [methyl-^{3}H] thymidine deoxyribose (TdR; Amersham Pharmacia Biotech, Inc., Piscataway, NJ) incorporation assay. The number of cells was counted using a hemocytometer at various times (0–120 h) after irradiation.

COMET ASSAY

A comet assay was performed to detect DNA migrating from single cells in the gel, following previously described methods with slight modifications [Son et al., 2009]. Briefly, MC3T3-E1 cells were exposed to 8 Gy radiation in the presence and absence of 200 μM DPDS-U. Cells were suspended in 1% low melting point agarose in PBS (pH 7.4) and aliquoted onto glass microscope slides at 24 h post-irradiation. The slides were placed in single rows and electrophoresed at 30 V (1 V/cm) and 300 mAmp for 30 min. Finally, the slides were washed with 0.4 M Tris (pH 7.5) at 4°C and stained with ethidium bromide.

CELL CYCLE PROGRESSION ANALYSIS

Cell cycle distribution was determined by flow cytometric analysis after propidium iodide (PI) staining as described elsewhere [Yu et al., 2010]. In brief, MC3T3-E1 cells were irradiated with 8 Gy in the presence of 200 μM DPDS-U and the cells were collected using a trypsin buffer after 24 h incubation. The cells were washed twice with PBS and the cell suspension (2×10^6 cells) was fixed with 70% ethanol at 4°C for 24 h. After a brief wash, cells were incubated overnight at 4°C with 500 μl of PI staining solution (50 μg/ml PI in a sample buffer containing 100 μg/ml RNase A) and 10,000 cells per experiment were analyzed using the FACS Calibur® system (Becton Dickinson).

MEASUREMENT OF INTRACELLULAR REACTIVE OXYGEN SPECIES (ROS)

A stock solution of 2′,7′-dichlorodihydrofluorescein-diacetate (DCFH-DA) (50 mM; Calbiochem, Darmstadt, Germany) was prepared in DMSO and stored at −20°C in the dark. MC3T3-E1 cells in 6-well culture plates (2×10^6 cells/well) were exposed to 8 Gy of radiation in the presence and absence of DPDS-U or NAC. At 12 h post-irradiation, the cells were washed with PBS and incubated at 37°C for an additional 1 h before treatment with 25 μM DCFH-DA for 20 min. The green fluorescence of 2′,7′-dichlorofluorescein (DCF) was recorded at 515 nm (FL 1) using a FACS Vantage® system (Becton Dickinson), and 10,000 events were counted per sample. The results were also expressed as the percentage increase relative to non-irradiated cells.

MEASUREMENT OF H_2O_2 IN CULTURE MEDIUM

H_2O_2 concentration in culture medium lacking FBS was determined using the colorimetric H_2O_2 detection kit (Assay Designs, Ann Arbor, MI) according to the protocols provided. In brief, MC3T3-E1 cells were incubated with 0.1 mM H_2O_2 in the presence and absence of DPDS-U or NAC. After co-incubation for 30 min, the concentration of H_2O_2 was calculated by measuring the absorbance of the purple solution at 550 nm.

MDA DETERMINATION AND LDH LEAKAGE ASSAY

The effect of DPDS-U on irradiation-mediated lipid peroxidation was determined 24 h post-irradiation by measuring intracellular malondialdehyde (MDA) levels as described elsewhere [Choi et al., 2010]. Briefly, cell lysates (100 μl per each sample) were mixed with 50 μl of 8% SDS and then with a buffer containing 20% acetic acid and 0.6% thiobarbituric acid. The mixtures were treated with a butanol:pyridine mixture (15:1, v/v) before centrifugation and MDA levels in the supernatants were measured at 532 nm using 1,1,3,3-tetraethoxypropane as a standard. Lactate dehydrogenase (LDH; EC 1.1.1.27) in the culture medium was measured at 24 h post-irradiation using an assay kit provided by Thermo Scientific (Rockford, IL) according to the manufacturer's instructions. The enzyme activity was expressed as units per liter.

MEASUREMENT OF INTRACELLULAR ANTIOXIDANT ACTIVITIES

MC3T3-E1 cells were exposed to 8 Gy of radiation in the presence of DPDS-U or NAC, collected at 24 h post-irradiation, and resuspended in a protein lysis buffer prior to cellular antioxidant activity determination. Reduced glutathione (GSH) content and superoxide dismutase (SOD) activity (EC 1.15.1.1) were measured using assay kits (#K264-100 for GSH and #K335-100 for SOD, BioVision Research Products, Mountain View, CA) according to the manufacturer's instructions. SOD activity was expressed as U/mg protein based on a SOD standard curve. Catalase (EC 1.11.1.6) activity was determined using the Amplex Red Catalase Assay Kit (A22180, Molecular Probes Inc., Eugene, OR).

REAL TIME RT-PCR

Total RNA was prepared from irradiated cells at 12 h post-irradiation using the SV Total RNA Isolation System (Promega, Madison, WI) and reverse-transcribed using an RNA PCR kit according to the

instruction manual (Access RT-PCR System, Promega). Real time RT-PCR amplification was performed using an ABI Prism 7900HT Sequence Detection System (Applied Biosystems, Foster, CA). The PCR primer sequences used [Arai et al., 2007; Lin et al., 2010] were as follows: 5′-aagaggctaagaccgccttc-3′ and 5′-gcataaattcccactgccac-3′ for heme oxygenase-1 (HO-1), 5′-ttagtcagcgacagaaggac-3′ and 5′-ccagttgaaactgagcgaaa-3′ for nuclear factor E2 p45-related factor 2 (Nrf2), and 5′-caccaccatggagaaggccg-3′ and 5′-gaacacggaaggc-catgcca-3′ for GAPDH. In addition, aliquots of a cDNA pool were subjected to PCR and amplified in a 20-μl reaction mixture using Taq polymerase and the gene-specific primers. Amplifications were performed with a DNA thermal cycler (model PTC-100, Perkin Elmer, Waltham, MA), and the resulting PCR products were electrophoresed on 1–2% agarose gels followed by ethidium bromide staining. Band intensity was calculated using a gel imaging system (model F1-F2 Fuses type T2A, BIO-RAD, Segrate, Italy).

WESTERN BLOT ANALYSIS

Nuclear, cytosolic, and whole proteins were obtained from MC3T3-E1 cells at various times after irradiation as described previously [Yu et al., 2011]. The amount of protein in the samples was quantified using the Bradford method. Equal amounts of protein (30 μg) were separated by 12% SDS–PAGE and blotted onto PVDF membranes. Blots were probed with primary antibodies and then incubated with horseradish peroxidase-conjugated anti-IgG in a blocking buffer for 1 h. The blots were developed with enhanced chemiluminescence (GE Healthcare, Buckinghamshire, UK) and exposed to X-ray film (Eastman-Kodak, Rochester, NY). Antibodies specific for cyclin B1, cyclin D1, cyclin E, p21, HO-1, Nrf2, Lamin B, and β-actin were purchased from Santa Cruz Biotechnology (Santa Cruz, CA).

HO-1 ACTIVITY ASSAY

This assay was performed as previously described [Yu et al., 2013]. In brief, lysates of MC3T3-E1 cells were prepared 24 h post-radiation and homogenates containing biliverdin reductase were obtained from rat liver. After quantifying protein concentration, cell lysates and homogenates were incubated with NADPH and hemin for 1 h, whereas blanks were reacted with hemin only. The concentration of bilirubin as the product of degradation by HO-1 was determined as the difference between absorbance at 450 and 530 nm using a microplate spectrophotometer (Bio-Tek, Inc., Winooski, VT). HO-1 activity was expressed as nmol/mg protein/h. MC3T3-E1 cells were also exposed to 200 μM DPDS-U, 2.5 mM NAC, or 0.1 mM H_2O_2 alone for 12 h and the respective HO-1 activity was compared.

SMALL INTERFERING RNA TRANSFECTION

Small interfering (si) RNA-mediated silencing of the Nrf2 gene was performed using siRNA duplexes purchased from Invitrogen (Carlsbad, CA) according to the manufacturer's protocol. An unrelated siRNA with random nucleotides was used as the non-silencing control. For transfection, MC3T3-E1 cells were seeded in six-well culture plates and transfected with siRNA duplexes using Lipofectamine 2000 (Invitrogen) according to the manufacturer's instructions. The cellular Nrf2 protein level was measured 24 h after transfection by immunoblotting.

STATISTICAL ANALYSIS

Unless specified otherwise, data are expressed as the means ± standard deviations (SD) from triplicate experiments with at least three samples per experiment. A one-way analysis of variance (SPSS version 12.0 software) followed by Scheffe's test was applied to determine the significance of differences between groups. A P value < 0.05 was considered significant.

RESULTS

DPDS-U SIGNIFICANTLY INHIBITS THE IRRADIATION-INDUCED DECREASE IN VIABILITY AND PROLIFERATION OF OSTEOBLASTS

We first explored the effects of irradiation on the viability and proliferation of MC3T3-E1 cells according to the dose and incubation time. Figure 1B shows a gradual reduction in cell number with increased irradiation intensity and culture time. Irradiation at doses greater than 4 Gy appeared to reduce the number of cells. Irradiation at 8 Gy significantly decreased cell viability and DNA synthesis by up to 61% and 68%, respectively, at 24 post-irradiation compared with non-irradiated cells (Fig. 1C). We examined the protective effects of PAPU compounds on irradiation-mediated cellular damage in MC3T3-E1 cells. Although several PAPU compounds at 200 μM protected against the irradiation (8 Gy)-mediated reduction in cell viability, DPDS-U had the greatest effect (Fig. 1D). There was no significant difference of viability between the untreated control and the irradiated cells with 8 Gy in the presence of 200 μM DPDS-U. Although DPDS-U at 200 μM also restored significantly the levels of viability and DNA synthesis reduced by the irradiation at 12 Gy, these levels in the cells combined with DPDS-U were still lower than that of the control cells (Fig. 1E). With this regard, we selected 8 Gy as the irradiation dose in subsequent experiments and further investigated the radioprotective effect of DPDS-U according to the concentrations added. Pretreatment with DPDS-U suppressed the irradiation-induced reduction in both viability (Fig. 1F) and DNA synthesis (Fig. 1G) in a dose-dependent manner. The protective effects of 200 μM DPDS-U were similar to those of 5 mM NAC and DPDS-U (200 μM) and NAC (5 mM) alone did not affect viability and DNA synthesis in MC3T3-E1 cells (Figs. 1F and G).

As the irradiation-mediated cellular damages are accompanied by oxidative stress, we evaluated the protective potential of PAPU compounds against glucose oxidase-mediated oxidative damage using a ROS-sensitive cell line, BJAB cell (Supplementary Fig. S1). Among the compounds, DPDS-U at 200 μM also showed the greatest protection on cytotoxicity (Supplementary Fig. 1A) and DNA damage (Supplementary Figs. 1B and C). Furthermore, DPDS-U at 200 μM did not cause any toxic effects on BJAB cells as well as primary cell cultures (Fig. 1H). Taken together, we selected 8 Gy and DPDS-U at 200 μM as the irradiation and compound dose in subsequent experiments to verify the mechanisms by which the compound exerts radioprotection in osteoblasts.

DPDS-U PREVENTS IRRADIATION-MEDIATED CHANGES IN CELL CYCLE PROGRESSION, ROS PRODUCTION, AND DNA DAMAGE IN MC3T3-E1 CELLS

The results from flow cytometric analysis revealed that irradiation at 8 Gy affected cell cycle progression by arresting cell populations in the G_2/M phase at 24 h post-irradiation (Fig. 2A). Calculation of the

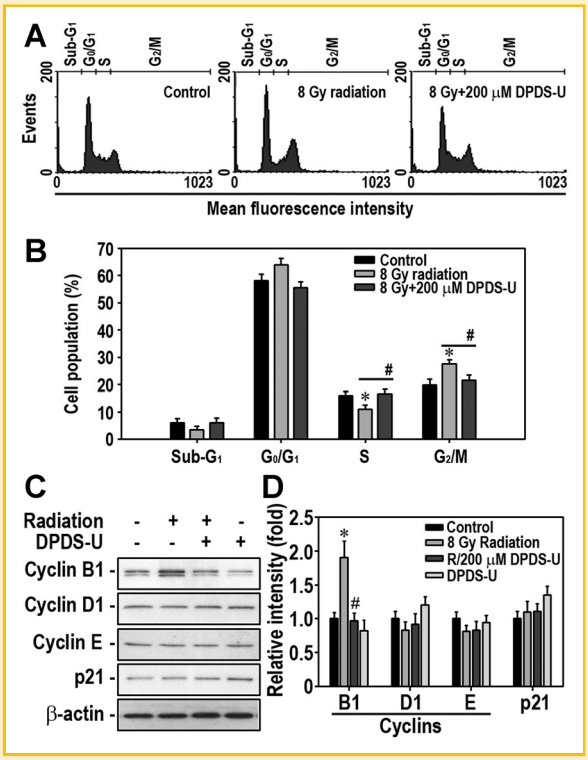

Fig. 2. Irradiation induces cell cycle arrest at the G_2/M phase with a concomitant reduction of the S phase population. MC3T3-E1 cells were exposed to 8 Gy of radiation in the presence and absence of 200 μM DPDS-U. A: At 24 h post-irradiation, cells were stained with PI and flow cytometric analysis was performed. B: The percentage of cells at each cell cycle stage was calculated from triplicate experiments. C: At the same time, whole protein lysates were prepared from the cells and then processed for Western blot analysis using antibodies specific for cyclin B1, cyclin D1, cyclin E, and p21. D: The relative intensity of these proteins was calculated from triplicate experiments after normalizing the bands to that of β-actin. $^{*}P < 0.05$ versus non-irradiated controls. $^{\#}P < 0.05$ versus 8 Gy irradiation only.

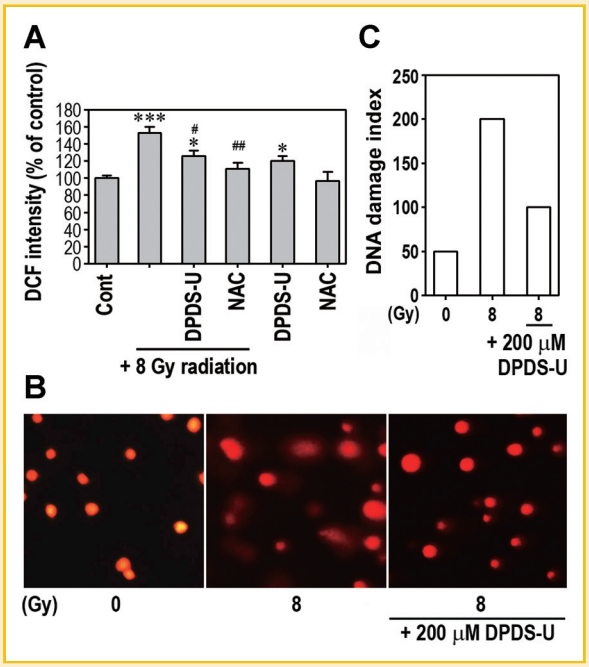

Fig. 3. DPDS-U suppresses irradiation-induced ROS production and DNA damage in MC3T3-E1 cells. A: Cells were stained with DCFH-DA and analyzed using flow cytometer at 12 h post-irradiation. The data represent the mean ± SD from triplicate experiments after calculating the flow cytometric signals using the WinMDI 2.9 program. $^{*}P < 0.05$ and $^{***}P < 0.001$ versus non-irradiated controls. $^{\#}P < 0.05$ and $^{\#\#}P < 0.01$ versus irradiation only. B: Aliquots of the cells were processed for the comet assay 24 h after irradiation. A representative image of ethidium bromide-stained nuclei from triplicate experiments is shown. C: More than 100 comets/treatment were sorted into five classes and the DNA damage index was calculated.

cell population at each stage of cell cycle progression from triplicate experiments revealed a significant decrease in the S phase population with concomitant increases in the G_2/M phases, whereas this change was not seen in cells that were incubated with DPDS-U (Fig. 2B). The results from Western blot analysis revealed the levels of cyclin B1, but not of p21, was significantly increased in the cells irradiated with 8 Gy and this increase was attenuated by treatment with 200 μM DPDS-U (Figs. 2C and D). A slight decrease of cyclin D1 and cyclin E levels was found in the irradiated cells, but there was no significant difference compared to the untreated control cells. DPDS-U itself did not affect the expression of both cyclins and p21 at a significant level. Flow cytometric analysis also showed an increase in intracellular ROS levels after 8 Gy irradiation (Fig. 3A). This increase was significantly diminished in the presence of 200 μM DPDS-U or 5 mM NAC; however, the DCF intensity in cells irradiated in the presence of DPDS-U was still higher than that in the non-irradiated control cells. This probably reflects a chemical property of DPDS-U because, unlike NAC, DPDS-U itself increased the DCF signal in the cells. The comet assay showed a higher level of single-strand break (SSB) formation in cells that were only irradiated compared with cells that were irradiated and treated with DPDS-U (Fig. 3B). When SSB formation was categorized into five classes (classes 0–4), the irradiation-induced DNA damage was clearly reduced by DPDS-U (Fig. 3C). Similar results were obtained when 5 mM NAC was added to the cells before irradiation (data not shown).

DPDS-U REVERSES THE INCREASE IN MDA AND LDH LEVELS AND THE DECREASE IN GSH AND SOD ACTIVITIES IN IRRADIATED MC3T3-E1 CELLS

Because LDH and MDA are specific markers for cellular damage, we examined the effect of DPDS-U on the generation of these markers in MC3T3-E1 cells at 24 h post-irradiation. Figure 4A shows the irradiation-mediated increase in MDA level and its inhibition by DPDS-U. In parallel with this, the radiation-mediated increase in LDH leakage was also significantly suppressed by pretreatment with 200 μM DPDS-U (Fig. 4B). Similarly, 5 mM NAC showed potent protective activity by inhibiting the irradiation-induced increase in MDA and LDH levels. Irradiation decreased the GSH level (Fig. 4C) and SOD activity (Fig. 4D), but not catalase activity (Fig. 4E), at 24 h post-irradiation. Pretreatment with 200 μM DPDS-U or 5 mM NAC almost completely restored the radiation-mediated reduction of GSH and SOD levels up to the level of non-treated control groups.

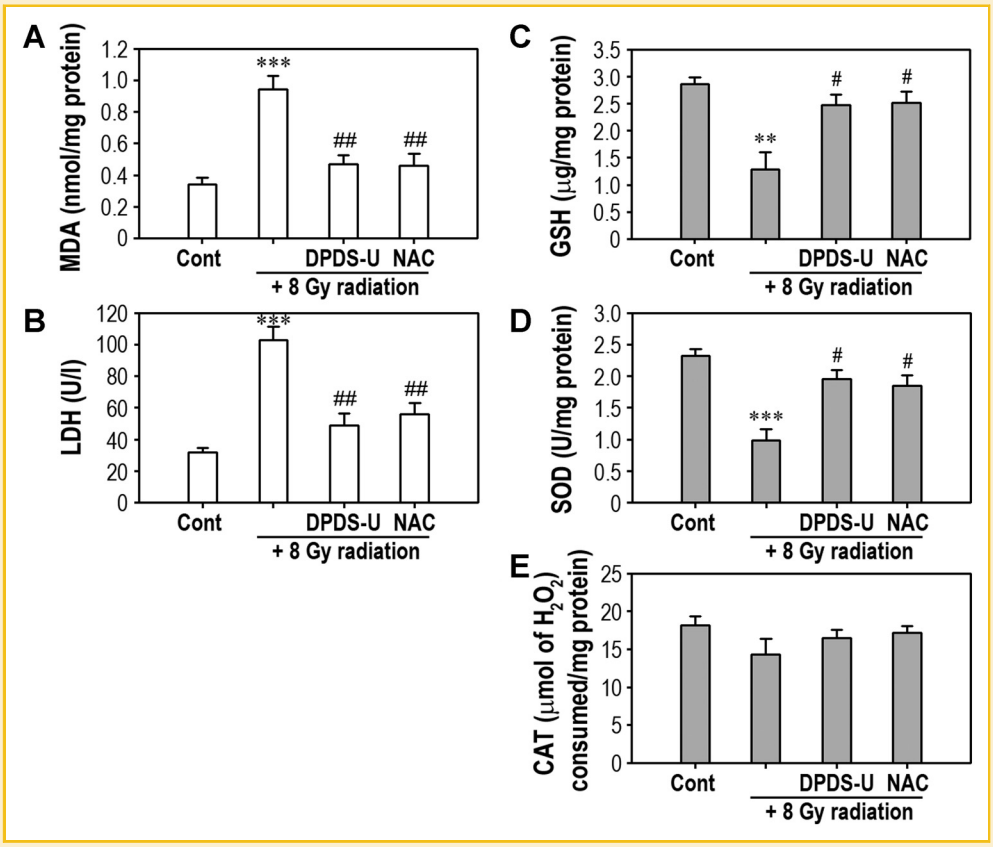

Fig. 4. DPDS-U inhibits irradiation-induced changes in the levels of MDA, LDH, GSH, and SOD. MC3T3-E1 cells were irradiated with 8 Gy in the presence of 200 μM DPDS-U or 5 mM NAC. At 24 h post-irradiation, the levels of MDA (A), LDH (B), GSH (C), SOD (D), and catalase (CAT) (E) were determined. $^{**}P < 0.01$ and $^{***}P < 0.001$ versus non-irradiated controls. $^{\#}P < 0.05$ and $^{\#\#}P < 0.01$ versus irradiation only.

DPDS-U ATTENUATES IRRADIATION-INDUCED CELLULAR DAMAGE BY ENHANCING HO-1 INDUCTION AND ACTIVITY IN OSTEOBLASTS

Based on the knowledge that HO-1 induction is increased under stress conditions and regulates various cellular events, we investigated the effect of DPDS-U on HO-1 induction at mRNA and protein levels in irradiated-MC3T3-E1 cells. Irradiation at 8 Gy increased HO-1 mRNA expression (Fig. 5A) and protein induction (Fig. 5B). Pretreatment with 200 μM DPDS-U did not inhibit the radiation-mediated increase in HO-1 mRNA and protein levels, but instead facilitated mRNA expression (Figs. 5C and D). In fact, DPDS-U itself significantly increased HO-1 induction at both mRNA and protein levels. These findings were supported by enzymatic assays, which showed that the radiation-induced increase in HO-1 activity was augmented in the presence of DPDS-U (Fig. 5E). We explored the roles of HO-1 in viability and lipid peroxidation in irradiated MC3T3-E1 cells by treatment with a selective inhibitor of HO-1, zinc protoporphyrin IX (ZnPP IX). The protective effect of 200 μM DPDS-U against the radiation-induced reduction in viability was not observed in the presence of 10 μM ZnPP IX (Fig. 5F). Similarly, addition of ZnPP IX blocked DPDS-U-mediated protection against the increase in MDA (Fig. 5G) and LDH levels (Fig. 5H) that occurred after irradiation.

Nrf2 PLAYS A CRITICAL ROLE IN PROTECTION AGAINST IRRADIATION-MEDIATED CELLULAR DAMAGE THROUGH UPREGULATION OF HO-1 INDUCTION

Because Nrf2 is known to be a critical regulator of HO-1 and protects cells against cellular stresses by maintaining normal levels of ROS, we explored whether Nrf2 is involved in DPDS-U-mediated radioprotection in osteoblasts. Irradiation at 8 Gy stimulated the translocation of Nrf2 into the nucleus and this was further accelerated by DPDS-U in a dose-dependent manner (Figs. 6A and B). Treatment with 200 μM DPDS-U alone also significantly increased the nuclear translocation of Nrf2. Real time RT-PCR analysis showed that irradiation and DPDS-U separately increased Nrf2 mRNA expression in MC3T3-E1 cells, and this was further increased by combining these agents (Fig. 6C). To clarify the role of Nrf2 in HO-1 expression and cellular damage in irradiated osteoblasts, we transfected MC3T3-E1 cells with Nrf2-specific siRNA. Western blot analysis confirmed a reduction in total Nrf2 protein level 24 h after transfection (Fig. 6D). Irradiation-mediated HO-1 induction and its facilitation by DPDS-U were attenuated by transfection with Nrf2 siRNA (Fig. 6E). The stimulation of HO-1 mRNA expression by irradiation, DPDS-U, or their combination was almost completely inhibited by transfection with Nrf2 siRNA (Fig. 6F). Furthermore, Nrf2 siRNA significantly diminished the

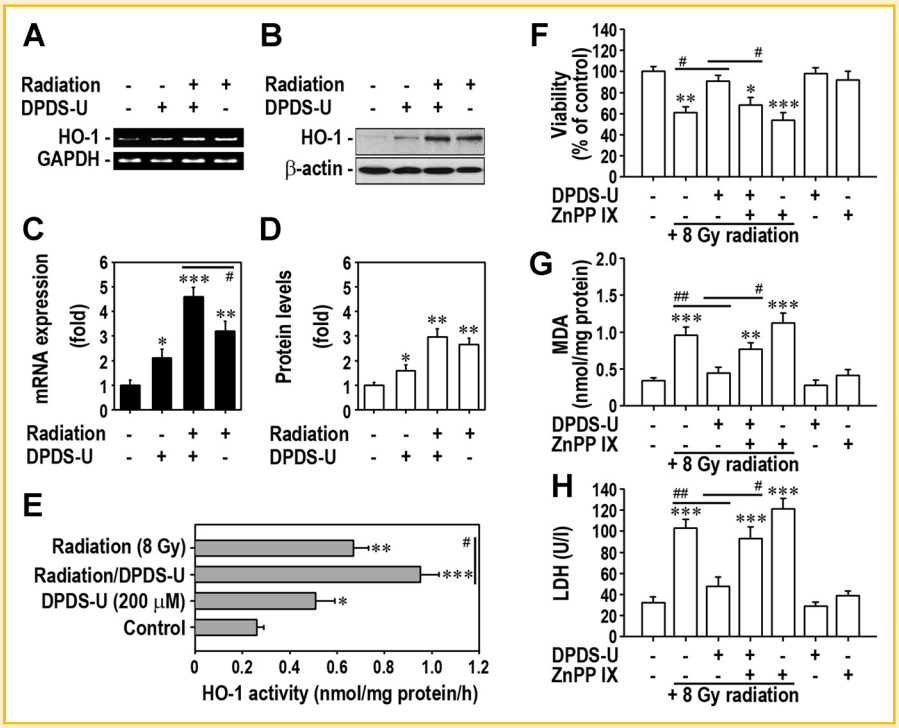

Fig. 5. HO-1 plays an important role in DPDS-U-mediated radioprotection. MC3T3-E1 cells were exposed to 8 Gy of radiation in the presence and absence of 200 μM DPSD-U. HO-1 expression at mRNA (A,C) and protein levels (B,D) was analyzed at 12 and 24 h post-irradiation, respectively. Panels C and D show the relative expression levels calculated form triplicate experiments. E: HO-1 activity in the cells was determined at 24 h post-irradiation. F,G,H: MC3T3-E1 cells were pretreated with 10 μM ZnPP IX and/or 200 μM DPDS-U before irradiation and cell viability (F) and levels of MDA (G) and LDH (H) were determined at 24 h post-irradiation. $^{*}P < 0.05$, $^{**}P < 0.01$, and $^{***}P < 0.001$ versus non-irradiated control values. $^{\#}P < 0.05$ and $^{\#\#}P < 0.01$ indicate significant differences between the experiments.

protective effect of DPDS-U against the irradiation-mediated decrease in cell viability (Fig. 6G).

IRRADIATION DIFFERENTIALLY ENHANCED Nrf2 NUCLEAR TRANSLOCATION AND HO-1 INDUCTION ACCORDING TO THE RADIATION DOSE

We further investigated the patterns of Nrf2 and HO-1 induction according to the dose of radiation or H_2O_2. Nrf2 nuclear translocation (Fig. 7A) and cellular HO-1 induction (Fig. 7B) were inversely proportional to the irradiation intensity (0–8 Gy), such that irradiation with 0.5 Gy led to a higher level of Nrf2 relocation and HO-1 induction than irradiation with 8 Gy at 6 h post-irradiation. Conversely, intracellular ROS levels were increased by irradiation in a dose-dependent manner, and cellular SOD activity and viability of the cells at 24 h post-irradiation were significantly reduced by exposure to 8 Gy (Supplementary Fig. S2A–C). When the cells were exposed to H_2O_2 (0–1 mM), the increase in HO-1 induction started at 0.05 mM, peaked by 0.1 mM, and gradually decreased at concentrations greater than 0.2 mM H_2O_2 (Fig. 7C). In parallel with this, viability of the cells was reduced after exposure to concentrations greater than 0.2 mM (Supplementary Fig. S2D). This suggested that HO-1 is induced in response to mild oxidative stress and mediates a survival signal, whereas excessive ROS accumulation predominantly causes a stress signal that eventually leads to cell death.

DPDS-U AND NAC REDUCE OXIDATIVE STRESS THROUGH DIFFERENT MECHANISMS

Both DPDS-U and NAC showed radioprotective effects in various experimental assays (Figs. 3 and 4), whereas only DPDS-U increased the DCF signal and HO-1 induction, indicating that it induced a change in the intracellular redox state. We analyzed HO-1 protein induction and activity following treatment with 200 μM DPDS-U, 5 mM NAC, and/or 0.1 mM H_2O_2. Treatment with DPDS-U, but not NAC, significantly increased the protein level (Fig. 8A) and activity (Fig. 8B) of HO-1 in MC3T3-E1 cells, although the increases were significantly lower than those induced by 0.1 mM H_2O_2. In co-treatment with H_2O_2, NAC significantly inhibited HO-1 induction but DPDS-U did not (Fig. 8C). Measurement of ROS levels in the culture medium of the cells 30 min after addition of 0.1 mM H_2O_2 showed that both DPDS-U and NAC significantly decreased H_2O_2 levels, but DPDS-U had a greater effect than NAC (Fig. 8D).

DISCUSSION

In this study we exposed MC3T3-E1 osteoblast cells to X-ray radiation at a dosage of 1.5 Gy/min using a radiotherapeutic linear accelerator. This radiation dosage is similar to that used clinically during radiotherapy. We compared the protective effects of DPDS-U with those of the antioxidant NAC. As shown by the decrease in viability and TdR uptake in irradiated osteoblasts, our present

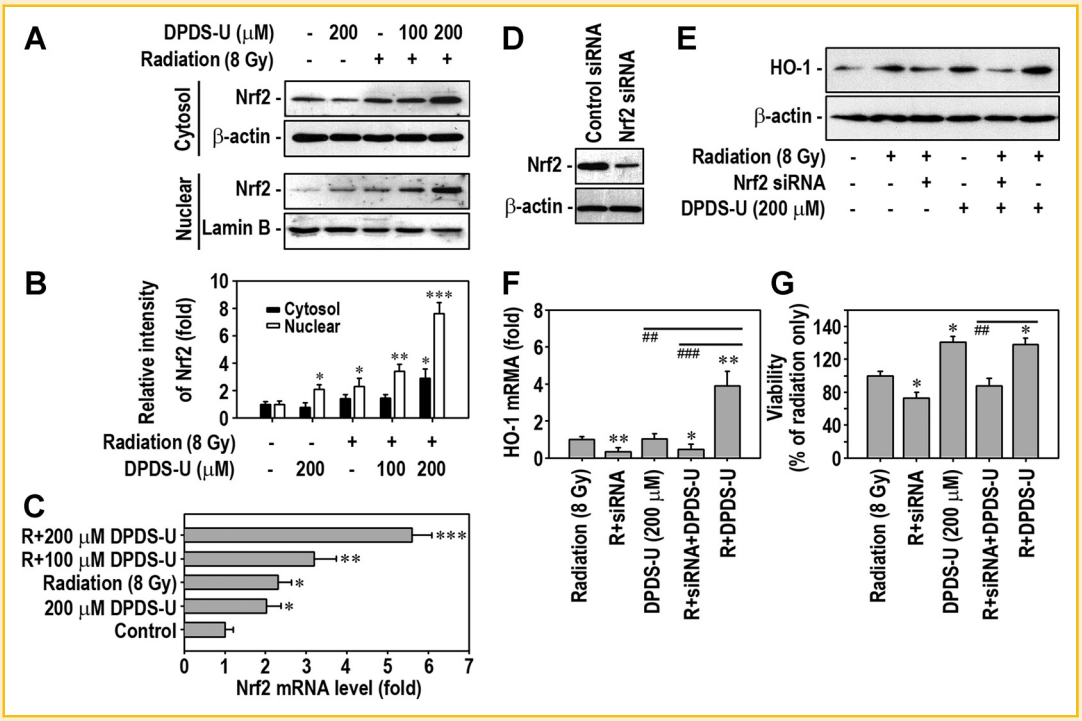

Fig. 6. DPDS-U activates HO-1 induction by the Nrf2 pathway in irradiated osteoblasts. MC3T3-E1 cells were exposed to 8 Gy of radiation with and without DPDS-U and at 6 h post-irradiation the protein level of cytosol and nuclear Nrf2 (A,B) and mRNA level of Nrf2 (C) were determined by Western blot and real time RT-PCR analyses, respectively. Panel B shows the relative intensity of Nrf2 protein from triplicate experiments. $^{*}P < 0.05$, $^{**}P < 0.01$, and $^{***}P < 0.001$ versus non-irradiated control values. E,G,F: MC3T3-E1 cells were transiently transfected with Nrf2-specific siRNA. Panel D shows the reduction in Nrf2 protein level 24 h after the transfection. After 24 h of transfection cells were exposed to 8 Gy of radiation in the presence of 200 μM DPSD-U. HO-1 protein induction (E) and cell viability (G), and HO-1 mRNA levels (F) were determined at 24 and 12 h post-irradiation, respectively. $^{*}P < 0.05$ and $^{**}P < 0.01$ versus 8 Gy irradiation only. $^{\#\#}P < 0.01$ and $^{\#\#\#}P < 0.001$ indicate significant differences between the experiments.

findings confirm that irradiation at a relatively high dose (>4 Gy) causes cellular damage. Although the effects of irradiation can be controversial depending on the dose and source of irradiation and the type of cells, numerous studies have shown that irradiation decreases DNA synthesis and/or viability in MC3T3-E1 cells [Matsumura et al., 1996; Gal et al., 2000; He et al., 2011], as well as in the murine osteoblast precursor cell line OCT-1 [Lau et al., 2010] and in newborn rat calvarial osteoblasts [Dare et al., 1997].

Oxidative damage to biomolecules is a well-known event in radiation-exposed cells [Kostyuk et al., 2012]. It was previously reported that exposure of MC3T3-E1 cells to irradiation at 15 mGy increased ROS levels and decreased expression of cyclin D1, even though this radiation dose did not affect cell viability or the expression of apoptotic markers [Pramojanee et al., 2012]. There are also reports that irradiation causes single- or double-strand DNA breaks in cells [Lau et al., 2010; Shinozaki et al., 2011] and cell cycle arrest at the G_2/M phase [Lau et al., 2010; Ho et al., 2011]. Consistent with these reports, our current data suggest that the irradiation induces intracellular ROS accumulation and this is closely associated with cell cycle arrest at the G_2/M phase. This was at least in part supported by the radiation-mediated increase of cyclin B1 and its reduction by DPDS-U in the MC3T3-E1 cells.

Following exposure to oxidative stress the primary cellular antioxidant defense systems, such as GSH, SOD, and catalase, play important protective roles by removing ROS and/or converting highly toxic radicals to non-toxic agents [Iborra et al., 2011]. In particular, cellular GSH levels are known to be a crucial factor in preventing oxidative damage, even after irradiation [Monga et al., 2011]. Although the mechanisms by which irradiation causes the depletion of cellular antioxidants are still unclear, ROS generation accompanied by mitochondrial stress is considered to play a central role both in the loss of cell function and the limitation of expression of cytoprotective genes in irradiated cells [Lee et al., 2010; Shin et al., 2013; Yu et al., 2013]. The decreased levels of these antioxidants may be also associated with their increased utilization for removing ROS increased after irradiation [Prasad et al., 2009]. This explains why antioxidants can protect cells against irradiation-induced damage. Accordingly, it is considered that irradiation induces ROS-mediated lipid peroxidation and reduces cellular antioxidant levels, leading to decreased cell viability and DNA synthesis and the appearance of DNA breaks, which will be effectively prevented by antioxidants such as DPDS-U.

The Nrf2/antioxidant response element (ARE) pathway is one of the most important contributors to cellular protection against numerous stresses, including oxidative stress [Shin et al., 2013]. AREs are located in the upstream promoter regions of various antioxidant genes including HO-1, which plays an important role in iron homeostasis as well as antioxidant defense in cells [Maines and Panahian, 2001]. There is considerable evidence supporting the role

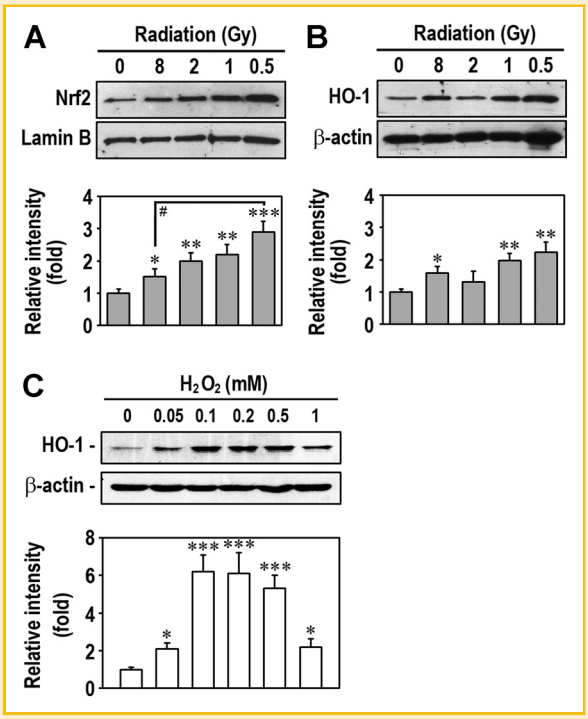

Fig. 7. Patterns of Nrf2 and HO-1 induction differ according to radiation dose or H_2O_2 concentration. MC3T3-E1 cells were exposed to various doses (0–8 Gy) of radiation and the protein levels of nuclear Nrf2 (A) and cytosolic HO-1 (B) were determined at 6 h post-irradiation. C: Cells were also exposed to the indicated doses of H_2O_2 and HO-1 protein induction was determined after 6 h of incubation. $^{*}P < 0.05$, $^{**}P < 0.01$, and $^{***}P < 0.001$ versus non-treated control values. $^{\#}P < 0.05$ versus the experiments.

of HO-1 as a potential target for the control of radiation-induced cellular damage [Lee et al., 2010]. The results of the present study reveal that exposure to irradiation or DPDS-U induces the endogenous antioxidative factor HO-1, and that Nrf2 is a critical upstream regulator of the DPDS-U-mediated induction of HO-1 in MC3T3-E1 cells. These data indicate that activation of the Nrf2/HO-1 pathway is closely associated with the radioprotective mechanism of DPDS-U.

There is considerable evidence supporting our present data that HO-1 is a specific marker of oxidative stress and its stimulation by antioxidants mediates cytoprotection against oxidative damage, even against irradiation-mediated injury [Lin et al., 2010; Chen et al., 2011; Shi et al., 2013; Yu et al., 2013]. The mechanism involved in the antioxidant-stimulated HO-1 induction is unclear, but it is considerable that antioxidants affect differently the expression of redox sensitive genes according to their chemical properties. We show here that treatment with DPDS-U alone, but not with NAC, slightly increased intracellular ROS in MC3T3-E1 cells, whereas DPDS-U reduced ROS levels in the culture medium of H_2O_2-exposed cells more efficiently than NAC. It is likely that a redox cycling activity of antioxidants is the main chemical property responsible for their dual potentials as antioxidant and prooxidant. This means that the redox cycling activity of a compound is proportional to its activity to stimulate ROS generation in cells. However, it is important to consider that a mild oxidative stress can activate a protective mechanism through Nrf2/HO-1 pathways, but severe ROS accumulation predominantly activate a stress signal related to cell death rather than survival signals. This suggests that antioxidants that produce high H_2O_2 levels may cause a stress signal, rather than a redox signal. The report that ascorbic acid, which has a high redox

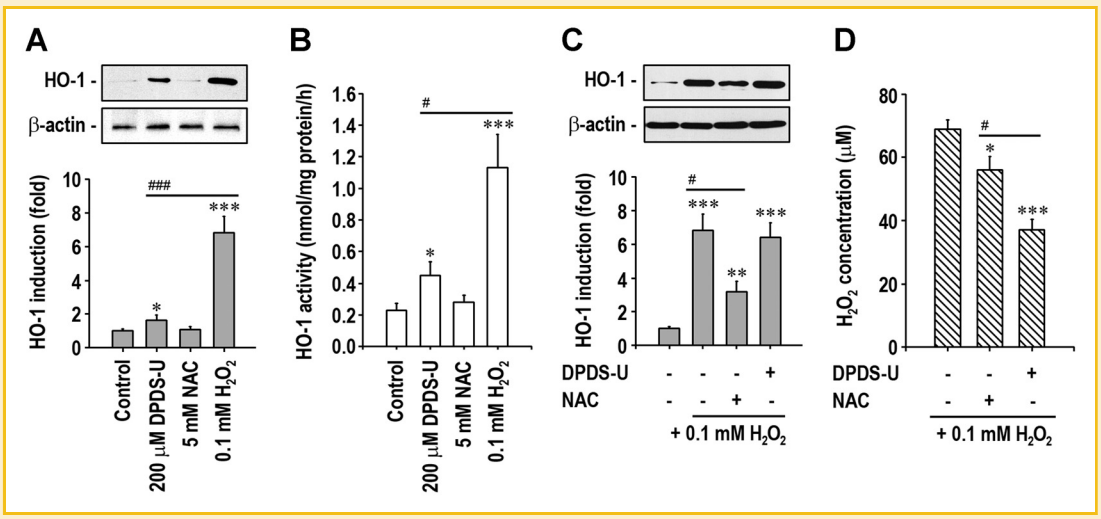

Fig. 8. DPDS-U and NAC have different effects on HO-1 induction in H_2O_2-treated MC3T3-E1 cells. Cells were incubated in the presence of either 200 μM DPDS-U, 5 mM NAC, or 0.1 mM H_2O_2, and HO-1 protein level (A) and activity (B) were determined after 6 and 12 h of incubation. C,D: Cells were treated with 0.1 mM H_2O_2 in the presence of 200 μM DPDS-U or 5 mM NAC. HO-1 protein induction (C) and H_2O_2 levels in the culture medium (D) were measured 6 h and 30 min after co-treatment, respectively. $^{*}P < 0.05$, $^{**}P < 0.01$, and $^{***}P < 0.001$ versus control values. $^{\#}P < 0.05$ and $^{\#\#\#}P < 0.001$ indicate significance differences between the experiments.

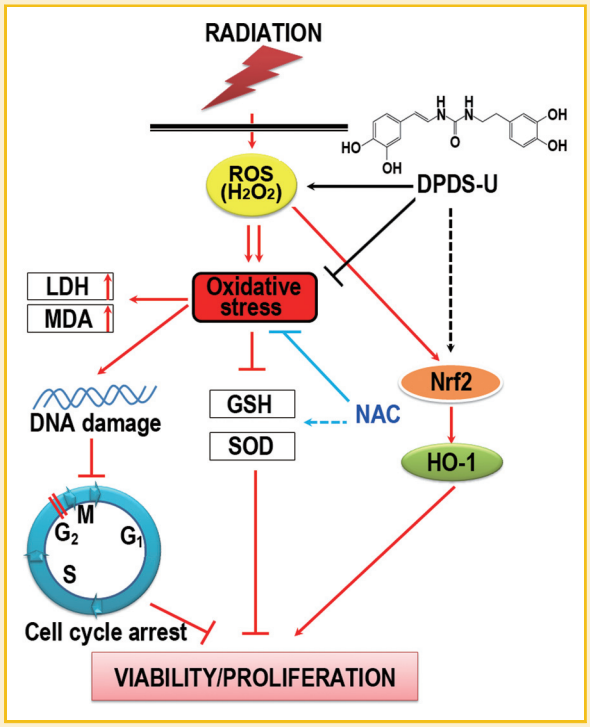

Fig. 9. Proposed mechanism of DPDS-U-mediated radioprotection in osteoblasts.

cycling activity, stimulated stress signals by producing excessive H_2O_2 and led to inactivation of Nrf2/HO-1 pathways supports our suggestion [Wagner et al., 2011]. Collectively, we suggest a mechanism for the action of DPDS-U: (1) DPDS-U itself may act as a prooxidant and induce low levels of intracellular ROS such as H_2O_2, thus affecting intracellular redox states and leading to subsequent activation of the Nrf2/HO-1 pathway; (2) under conditions of excessive ROS production, which can be caused by a relatively high dose of irradiation or direct H_2O_2 addition, DPDS-U predominantly acts as an antioxidant to control ROS levels, ultimately preventing cellular oxidative injury; and (3) the radioprotective mechanism of DPDS-U differs from that of NAC.

Although the present study has a limitation in emphasizing a clinical relevance of the DPDS-U due to the absence of in vivo study, its protective effect on H_2O_2-exposed cells greater than NAC, as well as the non-toxic effects of DPDS-U itself on various types of primary cells suggest the usefulness of the compound as a potent antioxidant. A chemical property of DPDS-U, which differs from that of NAC, might be due to its high redox cycling activity. It is important to note that a redox potential of antioxidant can be correlated with both the activities to regulate intracellular redox sensitive genes, such as Nrf2, HO-1, activator protein 1, and nuclear factor-κB, and to control oxidative stress by removing directly ROS and/or by stimulating antioxidant detoxifying enzymes [Sen and Packer, 1996; Kim et al., 2005; Granado-Serrano et al., 2010]. First of all, the efficiency of DPDS-U to protect irradiated cells was higher than NAC and other compounds examined; DPDS-U at 200 μM showed radioprotection similar to that of 5 mM NAC. Overall, we suggest that the great antioxidant and redox cycling activity with non-toxicity to normal cells will be the specific advantage of DPDS-U as compared with other antioxidant such as NAC.

In summary, this study demonstrates that DPDS-U can inhibit irradiation-induced cellular damage in osteoblasts. This beneficial effect is closely associated with its potential to eliminate excessive ROS accumulation and DNA damage, to restore the levels of GSH and SOD, and to activate Nrf2/HO-1 pathways in irradiated cells. Figure 9 shows a proposed mechanism by which DPDS-U exerts a radioprotective effect on osteoblasts. Further studies using an in vivo system will be needed to verify the mechanisms involved in DPDS-U-mediated radioprotection. In addition, it will be necessary to elucidate how DPDS-U interacts with survival signal molecules, especially with Nrf2/ARE-related factors.

ACKNOWLEDGEMENTS

This research was supported by Basic Science Program through the National Research Foundation of Korea (KRF) funded by the Ministry of Education, Science and Technology (2011-0010073 & NRF-2012R1A1B6001778).

REFERENCES

Arai M, Shibata Y, Pugdee K, Abiko Y, Ogata Y. 2007. Effects of reactive oxygen species (ROS) on antioxidant system and osteoblastic differentiation in MC3T3-E1 cells. IUBMB Life 59:27–33.

Chen JS, Huang PH, Wang CH, Lin FY, Tsai HY, Wu TC, Lin SJ, Chen JW. 2011. Nrf-2 mediated heme oxygenase-1 expression, an antioxidant-independent mechanism, contributes to anti-atherogenesis and vascular protective effects of *Ginkgo biloba* extract. Atherosclerosis 214:301–309.

Choi KC, Chung WT, Kwon JK, Yu JY, Jang YS, Park SM, Lee SY, Lee JC. 2010. Inhibitory effects of quercetin on aflatoxin B1-induced hepatic damage in mice. Food Chem Toxicol 48:2747–2753.

Dare A, Hachisu R, Yamaguchi A, Yokose S, Yoshiki S, Okano T. 1997. Effects of ionizing radiation on proliferation and differentiation of osteoblast-like cells. J Dent Res 76:658–664.

Gal TJ, Munoz-Antonia T, Muro-Cacho CA, Klotch DW. 2000. Radiation effects on osteoblasts in vitro: A potential role in osteoradionecrosis. Arch Otolaryngol Head Neck Surg 126:1124–1128.

Granado-Serrano AB, Martín MA, Haegeman G, Goya L, Bravo L, Ramos S. 2010. Epicatechin induces NF-κB, activator protein-1 (AP-1) and nuclear transcription factor erythroid 2p45-related factor-2 (Nrf2) via phosphatidylinositol-3-kinase/protein kinase B (PI3K/AKT) and extracellular regulated kinase (ERK) signalling in HepG2 cells. Br J Nutr 103:168–179.

He J, Qiu W, Zhang Z, Wang Z, Zhang X, He Y. 2011. Effects of irradiation on growth and differentiation-related gene expression in osteoblasts. J Craniofac Surg 22:1635–1640.

Ho SY, Wu WJ, Chiu HW, Chen YA, Ho YS, Guo HR, Wang YJ. 2011. Arsenic trioxide and radiation enhance apoptotic effects in HL-60 cells through increased ROS generation and regulation of JNK and p38 MAPK signaling pathways. Chem Biol Interact 193:162–171.

Hwang JM, Yu JY, Jang YO, Kim BT, Hwang KJ, Jeon YM, Lee JC. 2010. A phenolic acid phenethyl urea compound inhibits lipopolysaccharide-induced production of nitric oxide and pro-inflammatory cytokines in cell culture. Int Immunopharmacol 10:526–532.

Iborra M, Moret I, Rausell F, Bastida G, Aguas M, Cerrillo E, Nos P, Beltrán B. 2011. Role of oxidative stress and antioxidant enzymes in Crohn's disease. Biochem Soc Trans 39:1102–1106.

Kim JH, Jang YO, Kim BT, Hwang KJ, Lee JC. 2009. Induction of caspase-dependent apoptosis in melanoma cells by the synthetic compound (E)-1-(3,4-dihydroxyphenethyl)-3-styrylurea. BMB Rep 42:806–811.

Kim KA, Lee SA, Kim KH, Lee KS, Lee JC. 2013. Acteoside inhibits irradiation-mediated decreases in the viability and DNA synthesis of MC3T3-E1 cells. Food Sci Biotechnol 22:845–851.

Kim SS, Son YO, Chun JC, Kim SE, Chung GH, Hwang KJ, Lee JC. 2005. Antioxidant property of an active component purified from the leaves of paraquat-tolerant *Rehmannia glutinosa*. Redox Rep 10:311–318.

King AD, Griffith JF, Abrigo JM, Leung SF, Yau FK, Tse GM, Ahuja AT. 2010. Osteoradionecrosis of the upper cervical spine: MR imaging following radiotherapy for nasopharyngeal carcinoma. Eur J Radiol 73:629–635.

Kostyuk SV, Ermakov AV, Alekseeva AY, Smirnova TD, Glebova KV, Efremova LV, Baranova A, Veiko NN. 2012. Role of extracellular DNA oxidative modification in radiation induced bystander effects in human endotheliocytes. Mutat Res 729:52–60.

Lau P, Baumstark-Khan C, Hellweg CE, Reitz G. 2010. X-irradiation-induced cell cycle delay and DNA double-strand breaks in the murine osteoblastic cell line OCT-1. Radiat Environ Biophys 49:271–280.

Lee JC, Kinniry PA, Arguiri E, Serota M, Kanterakis S, Chatterjee S, Solomides CC, Javvadi P, Koumenis C, Cengel KA, Christofidou-Solomidou M. 2010. Dietary curcumin increases antioxidant defenses in lung, ameliorates radiation-induced pulmonary fibrosis, and improves survival in mice. Radiat Res 173:590–601.

Lin TH, Tang CH, Hung SY, Liu SH, Lin YM, Fu WM, Yang RS. 2010. Upregulation of heme oxygenase-1 inhibits the maturation and mineralization of osteoblasts. J Cell Physiol 222:757–768.

Maines MD, Panahian N. 2001. The heme oxygenase system and cellular defense mechanisms. Do HO-1 and HO-2 have different functions. Adv Exp Med Biol 502:249–272.

Matsumura S, Jikko A, Hiranuma H, Deguchi A, Fuchihata H. 1996. Effect of X-ray irradiation on proliferation and differentiation of osteoblast. Calcif Tissue Int 59:307–308.

Monga J, Sharma M, Tailor N, Ganesh N. 2011. Antimelanoma and radioprotective activity of alcoholic aqueous extract of different species of Ocimum in C(57)BL mice. Pharm Biol 49:428–436.

Pramojanee SN, Pratchayasakul W, Chattipakorn N, Chattipakorn SC. 2012. Low-dose dental irradiation decreases oxidative stress in osteoblastic MC3T3-E1 cells without any changes in cell viability, cellular proliferation and cellular apoptosis. Arch Oral Biol 57:252–256.

Prasad NR, Jeyanthimala K, Ramachandran S. 2009. Caffeic acid modulates ultraviolet radiation-B induced oxidative damage in human blood lymphocytes. J Photochem Photobiol B 95:196–203.

Schultze-Mosgau S, Lehner B, Rödel F, Wehrhan F, Amann K, Kopp J, Thorwarth M, Nkenke E, Grabenbauer G. 2005. Expression of bone morphogenic protein 2/4, transforming growth factor-beta1, and bone matrix protein expression in healing area between vascular tibia grafts and irradiated bone-experimental model of osteonecrosis. Int J Radiat Oncol Biol Phys 61:1189–1196.

Sen CK, Packer L. 1996. Antioxidant and redox regulation of gene transcription. FASEB J 10:709–720.

Shi Y, Liang XC, Zhang H, Wu QL, Qu L, Sun Q. 2013. Quercetin protects rat dorsal root ganglion neurons against high glucose-induced injury in vitro through Nrf-2/HO-1 activation and NF-κB inhibition. Acta Pharmacol Sin 34:1140–1148.

Shin SM, Yang JH, Ki SH. 2013. Role of the Nrf2-ARE pathway in liver diseases. Oxid Med Cell Longev 2013:763257.

Shinozaki K, Hosokawa Y, Hazawa M, Kashiwakura I, Okumura K, Kaku T, Nakayama E. 2011. Ascorbic acid enhances radiation-induced apoptosis in an HL60 human leukemia cell line. J Radiat Res 52:229–237.

Singh PK, Wise SY, Ducey EJ, Fatanmi OO, Elliott TB, Singh VK. 2012. α-Tocopherol succinate protects mice against radiation-induced gastrointestinal injury. Radiat Res 177:133–145.

Son YO, Kook SH, Choi KC, Jang YS, Jeon YM, Kim JG, Lee KY, Kim J, Chung MS, Chung GH, Lee JC. 2006. Quercetin, a bioflavonoid, accelerates TNF-α-induced growth inhibition and apoptosis in MC3T3-E1 osteoblastic cells. Eur J Pharmacol 529:24–32.

Son YO, Kook SH, Jang YS, Shi X, Lee JC. 2009. Critical role of poly (ADP-ribose) polymerase-1 in modulating the mode of cell death caused by continuous oxidative stress. J Cell Biochem 108:989–997.

Ueno T, Yamada M, Igarashi Y, Ogawa T. 2011. *N*-acetyl cysteine protects osteoblastic function from oxidative stress. J Biomed Mater Res A 99:523–531.

Wagner AE, Boesch-Saadatmandi C, Breckwoldt D, Schrader C, Schmelzer C, Döring F, Hashida K, Hori O, Matsugo S, Rimbach G. 2011. Ascorbic acid partly antagonizes resveratrol mediated heme oxygenase-1 but not paraoxonase-1 induction in cultured hepatocytes– Role of the redox-regulated transcription factor Nrf2. BMC Complement Altern Med 11:1.

Wambi C, Sanzari J, Wan XS, Nuth M, Davis J, Ko YH, Sayers CM, Baran M, Ware JH, Kennedy AR. 2008. Dietary antioxidants protect hematopoietic cells and improve animal survival after total-body irradiation. Radiat Res 169:384–396.

Yu JY, Kim JH, Kim TG, Kim BT, Jang YS, Lee JC. 2010. (*E*)-1-(3,4-Dihydroxyphenethyl)-3-styrylurea inhibits proliferation of MCF-7 cells through G_1 cell cycle arrest and mitochondria-mediated apoptosis. Mol Cells 30:303–310.

Yu JY, Zheng ZH, Son YO, Shi X, Jang YO, Lee JC. 2011. Mycotoxin zearalenone induces AIF- and ROS-mediated cell death through p53- and MAPK-dependent signaling pathways in RAW264.7 macrophages. Toxicol In Vitro 25:1654–1663.

Yu J, Zhu X, Qi X, Che J, Cao B. 2013. Paeoniflorin protects human EA.hy926 endothelial cells against gamma-radiation induced oxidative injury by activating the NF-E2-related factor 2/heme oxygenase-1 pathway. Toxicol Lett 218:224–234.

SUPPORTING INFORMATION

Additional supporting information may be found in the online version of this article at the publisher's web-site.